Microstructural, mechanical, and oxidation property evolution of gamma-TiAl alloy with addition of precious metals

by I.A. Mwamba*†, L.A. Cornish†, and E. van der Lingen*

Synopsis

Titanium aluminide of composition Ti-47.5 at.% Al was prepared by melting titanium and aluminium of commercial purity with additions of precious metals of 0, 0.2, 1, 1.5 and 2 at.% content. The microstructure, hardness and oxidation properties were assessed. It was found that at 47.5 at.% Al, the microstructure of plain TiAl alloys was duplex, consisting of duplex lamellar grains and γ grains. The lamellar grains consisted of alternating lamellae of γ (TiAl) and α_2 (Ti_3Al), with overall aluminium content in the range of 43–47 at.%. The γ grains had a aluminium content above 50 at.%. The addition of precious metals to the TiAl alloy resulted in the formation of a new phase, with a high precious metal content, occurring mostly in the γ phase, without any major change to the microstructure. Increasing the amount of precious metals resulted in an increase of the new phase amount, at the expense of the γ phase. The hardness of the different alloys was around $300HV_{10}$. Overall, the research has shown that addition of precious metals to TiAl resulted in a slight increase in hardness and a significant improvement of the oxidation resistance. This shows that alloying TiAl with precious metals, at the addition levels investigated, does not alter the mechanical properties very much, but improves oxidation resistance.

Keywords
Titanium aluminide, TiAl, precious metals, ternary alloys, microstructure, properties.

Introduction

TiAl is one of the titanium aluminides found in the Ti-Al system, which exists over a range of compositions. Titanium aluminides represent an important class of alloys, providing a unique set of mechanical and physical properties with high potential in the automotive industry, power plant turbines, and aircraft engines. Intensive research efforts over the past three decades have matured the knowledge on TiAl-based alloys, and this state of progress is currently encouraging the consideration of this class of materials for structural, automotive, and aerospace applications. The outstanding thermo-physical properties of these alloys result mainly from a strongly ordered structure, which confers the following beneficial properties: high melting point, low density in the range 3.9–4.2 g/cm[3], high elastic modulus, low diffusion coefficient, good structural stability, and high ignition temperature when compared to conventional titanium alloys[1]. TiAl-based alloys show superior specific strength-temperature properties compared to classical titanium alloys, steels, and nickel-based superalloys in the temperature range from 500 to 900°C. With all these advantages over conventional high-performance alloys, TiAl alloys have been seen as promising for high-temperature structural applications. However, the lack of room-temperature ductility is still the main obstacle to their utilization as engineering materials[2]. The rigid bond structure restricts the ability to accommodate plastic deformation, thus reducing ductility.

TiAl-based alloys display dramatically different microstructures depending on the composition near a 50:50 Ti:Al atomic ratio. While γ-TiAl is found in the aluminium-rich region alloys, titanium-rich alloys exhibit a two-phase microstructure, consisting of layers of ordered face-centred tetragonal TiAl with a $L1_0$ structure and close-packed hexagonal Ti_3Al with DO_{19}[3–4].

The γ-TiAl ($L1_0$, tP4) phase is an ordered, equiatomic compound of the light elements Ti and Al. The high aluminium content of this compound increases the resistance to oxidation and burning, two critical concerns in the use of titanium-based materials. Gamma TiAl remains ordered to melting at ~1 440°C. The strong Ti-Al bond leads to high activation energy for diffusion, which helps retain strength and resist creep at high temperatures when diffusion becomes the rate-controlling process.

* *Advanced Materials Division, Mintek.*

† *School of Chemical and Metallurgical Engineering and DST/NRF Centre of Excellence in Strong Materials, University of the Witwatersrand.*

 This paper was first presented at the ZrTa2011 New Metals Development Network Conference, 12–14 October 2011, Mount Grace Country House & Spa, Magaliesburg.

TiAl has a low resistance to oxidation at temperatures above 800°C. To date, many attempts have been made to improve the high-temperature oxidation resistance of stoichiometric TiAl, which include the sputtering of an Al film and subsequent interdiffusion treatment at 600°C for 24 hours in a high vacuum[5], sputtering of an Ag-containing TiAl coating[6], and insertion of silicon in the coating material of TiAl[7]. The beneficial influence of the coatings on the heat resistance of the alloy is a result of the presence of an aluminium-rich silicon-modified $TiAl_3$ phase, which is the most oxidation-resistant phase in the TiAl system[8].

A number of refractory metals have been found to significantly improve the oxidation resistance of γ-based materials, and these include Nb, W, and Cr[9]. Silver was also added to TiAl with a significant improvement of the oxidation resistance by promoting the formation of a continuous external alumina based scale[10,11]. In this work, precious metals including ruthenium, palladium, platinum, gold, and silver were added to TiAl-based alloy and the alloy was characterized in terms of microstructural evolution, hardness, and oxidation behaviour.

Experimental procedure

Preparation of TiAl compound

The TiAl alloy was prepared by melting titanium grade 2 and aluminium of commercial purity in a button arc furnace under argon. The target composition was Ti-47.5 at.% Al. Two types of alloys were prepared: plain TiAl and precious metals-containing TiAl. The compositions of the first set of melts at 0.2 at.% PMs (precious metals) are given in Table I. In the second set of melts, the amount of precious metals was increased to 1.0, 1.5, and 2.0 at.% at the expense of the titanium content, the aluminium content remaining 47.5 at.%.

Characterization of the benchmark alloys

The samples from the melting were cut, prepared metallographically, and observed with optical and scanning electron microscopes (SEM). SEM imaging and energy dispersive X-ray spectroscopy (EDX) were conducted with the FEI Nova NanoSEM®, a high-resolution scanning electron microscope (HR-SEM). The chemistry of the samples and the phases were determined using a combination of X-ray diffraction (XRD) and EDX.

For XRD, the samples were analysed with a PANalytical X'Pert Pro powder diffractometer with an X'Celerator detector and variable divergence with fixed receiving slits and Fe-filtered Co-Kα radiation. Phase identification was conducted using X'Pert Highscore plus software.

The plain TiAl and precious metals-containing compounds were heat treated in a tube furnace under argon flow. The samples were heated at a rate of 10°C/min to 1 000°C, then held for 1 hour and furnace-cooled. After heat treatment, the samples were characterized in terms of microstructure and hardness.

The oxidation behaviour of samples was determined by thermogravimetric analysis (TGA) using a NETZSCH STA instrument. TGA was conducted in air on the samples and the weight gain was deducted. The TGA has also allowed the determination of the onset of weight increase, corresponding to the onset of oxidation. Samples of 10 mg were loaded in the STA and heated from room temperature to 1 050°C under a flow of air.

Results and discussion

Microstructural characterization of cast alloys

Microstructure of TiAl with addition of 0.2 at.% precious metals

XRD analysis was conducted to evaluate the phase formation after melting of precursor materials in the button arc furnace. Titanium and aluminium were melted together and then remelted with ruthenium, platinum, palladium, gold, or silver addition. For comparison purposes, commercial TiAl in powder form was also scanned.

Typical XRD results are presented in Figures 1 to 3. For commercial TiAl powder (Figure 1), only TiAl peaks were clearly defined as the powder consisted of TiAl particles only. In the case of melted plain TiAl (Figure 2), there were TiAl peaks (γ) as well as Ti_3Al (α_2) peaks. These two phases were expected, as the composition was selected to produce a TiAl alloy with a duplex structure, consisting of lamellar and γ-TiAl grains. No titanium or aluminium peaks were observed, indicating complete alloying.

In the case of precious metals-containing TiAl at an addition of 0.2 at.% PMs (Ru, Pt, Pd, Au, or Ag), TiAl peaks appeared with a slight shift towards smaller Bragg angles, indicative of solid solution. Ti_3Al peaks were also visible on the XRD patterns. Again, no Al, Ti, or elemental precious metal peaks were visible. Peaks of elemental precious metals were not expected, given the low additions. The duplex

Table I

Elemental composition of the alloys

Compound	Composition (at.%)							
	Ti	Al	Ru	Pd	Pt	Ir	Ag	Au
Plain TiAl	52.5	47.5	-	-	-	-	-	-
Ru-containing TiAl	52.3	47.5	0.2	-	-	-	-	-
Pd-containing TiAl	52.3	47.5	-	0.2	-	-	-	-
Pt-containing TiAl	52.3	47.5	-	-	0.2	-	-	-
Ir-containing TiAl	52.3	47.5	-	-	-	0.2		-
Ag-containing TiAl	52.3	47.5	-	-	-	-	0.2	-
Au-containing TiAl	52.3	47.5	-	-	-	-	-	0.2

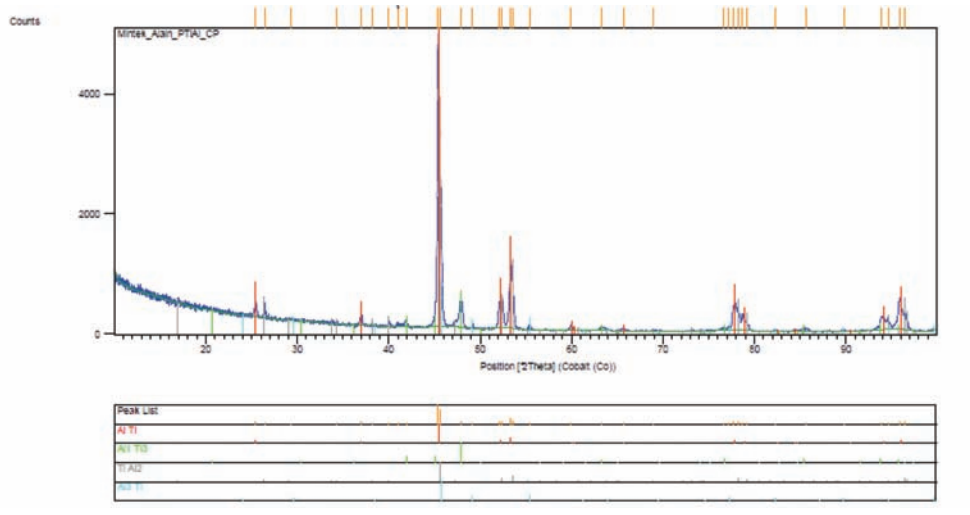

Figure 1—XRD pattern of commercial TiAl powder

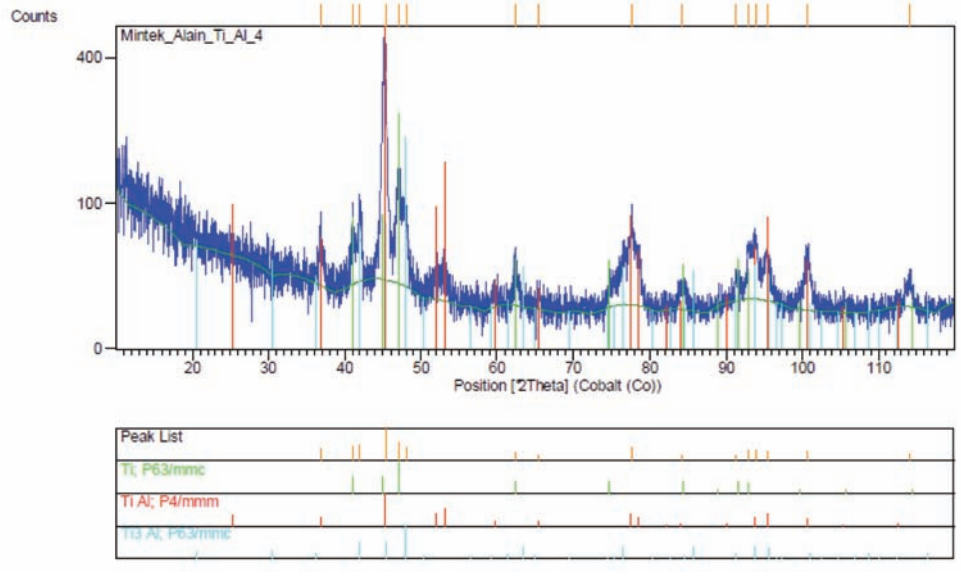

Figure 2—XRD pattern of as-cast plain TiAl

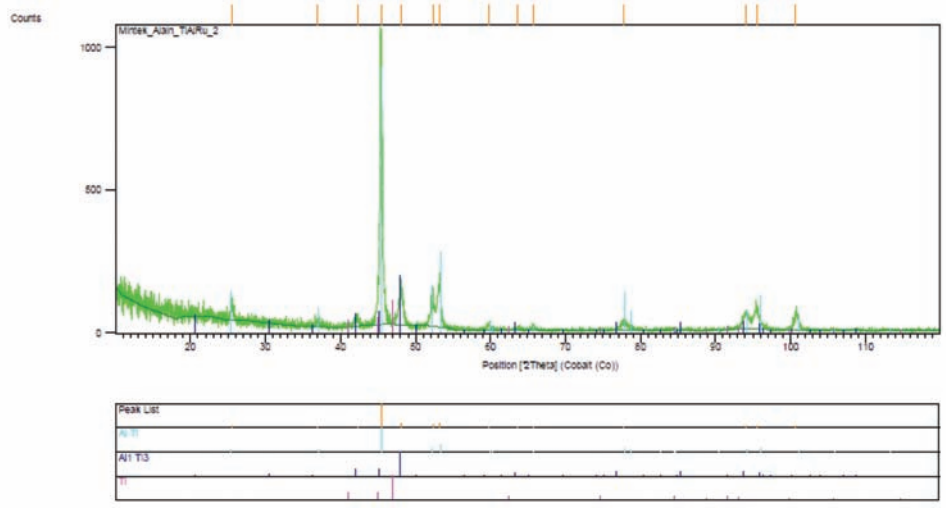

Figure 3—XRD pattern of as-cast TiAl with 0.2 at.% Ru

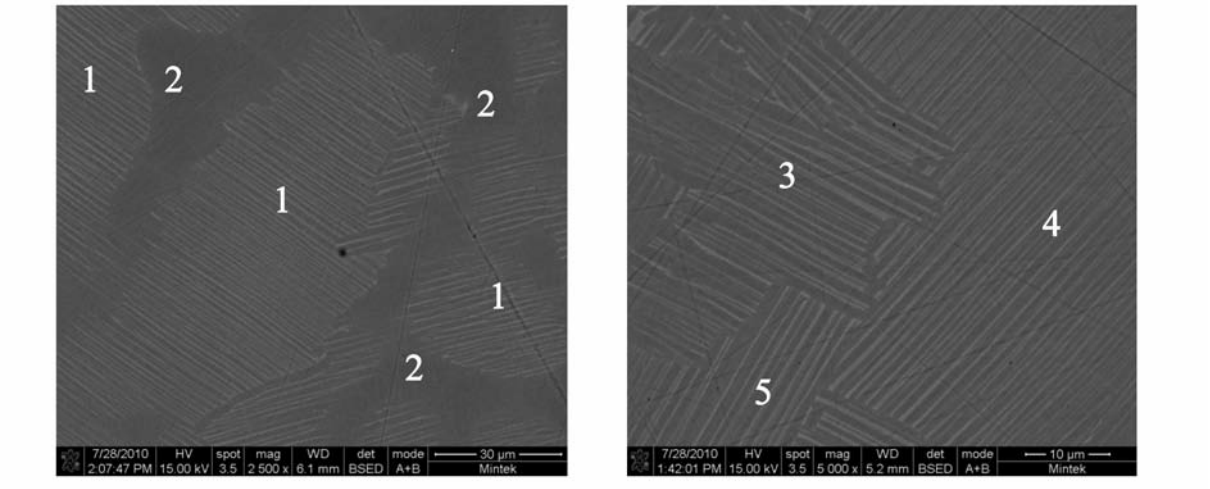

Figure 4—SEM mode micrograph of plain TiAl showing Ti_3Al and γ-TiAl phases

microstructure in the plain TiAl alloy is shown in Figure 4. The XRD patterns of Pt, Pd, Ag, and Au-containing TiAl alloys, which are not presented, showed similar peak trends, with Ti_3Al and γ-TiAl peaks.

Figure 4a shows that the microstructure obtained in plain TiAl at a target composition of Ti-47.5 at.% Al was duplex, consisting of lamellar grains (areas 1) with single-phase regions between them (areas 2). The grains identified in areas 1 comprised alternating light and dark lamellae.

In some parts, lamellar grains were adjacent. Figure 4b shows, at higher magnification, such an area which appears to be lamellar only. This figure also shows that different grains could be identified by the orientation of their lamellae (Areas 3 to 5).

Typical results obtained from EDX are reported in Table II. The overall composition indicates the formation of a duplex TiAl compound. After melting, the samples were furnace-cooled (a fairly slow cooling). The elemental composition showed that areas 1 in Figure 4a comprised alternating Ti_3Al (α_2) and γ-TiAl. According to the Ti-Al phase diagram[12], shown in Figure 5, Ti_3Al has an aluminium content of between 22 and 35 at.% at 400°C. From 35 to 49 at.% Al is the composition range of a two-phase field of Ti_3Al and TiAl, which was the case in these samples, with the lamellar region having a composition of 47.7 at.% Al. In the single-phase regions (areas 2 in Figure 4a), the aluminium content was above 50 at.%, showing the presence of only γ-TiAl. These observations indicated that the microstructure was a mixture of lamellar grains (with alternating α_2 and γ parallel phases) and γ-TiAl grains between the lamellar grains, typical of duplex microstructure[9].

Table II

EDX analysis of plain TiAl

Plain TiAl	Area	Elemental composition (at.%)			
		Ti	Std. dev.	Al	Std. dev.
	Overall	51.5	1.2	48.5	1.3
	Duplex 1	52.0	0.4	48.0	0.4
	Plain 2	47.7	1.1	52.3	1.2

SEM and EDS were also conducted on the TiAl compounds containing 0.2 at.% precious metals. Typical results are presented in Figure 6 and Table III respectively. SEM showed (Figure 6a) that the duplex structure was maintained in all samples in spite of the ruthenium addition. In addition, the precipitation of a light phase was observed in all samples doped with precious metals, mainly between the interfaces of the single-phase and duplex regions. The shape of these precipitates was irregular with no particular trend. No light phase was observed in the α_2/γ lamellar grains.

EDS results (Table III) showed that the light phases contained a higher precious metal content than the lamellar and γ phases. From Table III, the typical Ru content observed in the lamellar grains and γ-TiAl was below 1 at.%, which is in the range reported by Khataee *et al.*[13]. In a constitutional study of the Ti-Al-Ru system, they concluded that the solubility of ruthenium in γ is higher than in the lamellar phase, with reported values of about 0.5 at.% Ru in α_2 (Ti_3Al) and less or equal to 1 at.% in γ-TiAl.

The Al-Ru-Ti isothermal section in Figure 7 shows that the light phase reported in Table III (6.3 at.% Ru) is located in the zone containing γ-TiAl and the G-phase although the analysis of this small phase would have been affected by the surrounding phases. The G-phase is the $Al_{16}Ru_8Ti_6$ ternary

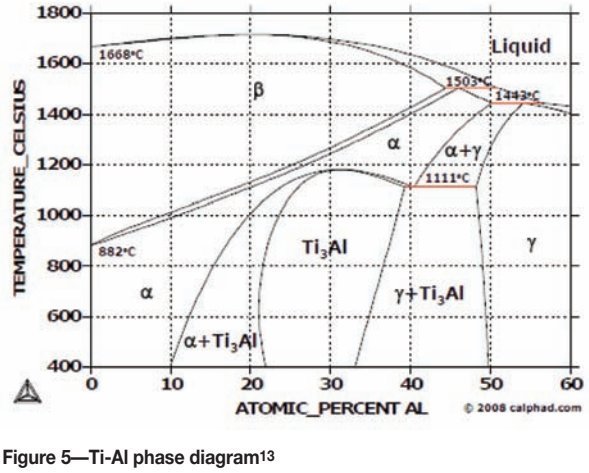

Figure 5—Ti-Al phase diagram[13]

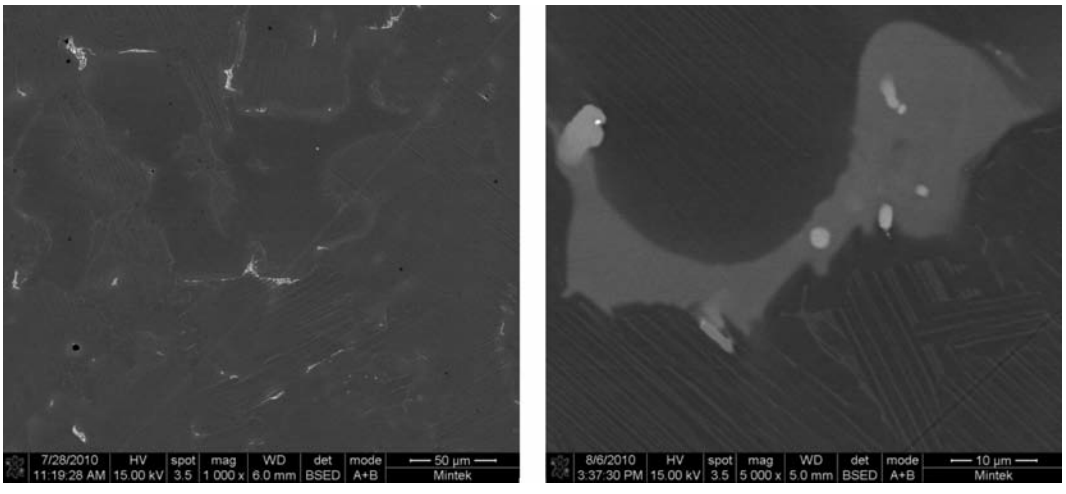

Figure 6—SEM mode micrographs of TiAl alloy with 0.2 at.% Ru

Table III

Typical EDX analysis of PMs-containing TiAl (5 analyses)

Alloy	Area	Elemental composition (at.%)					
TiAl-Ru		Ti	Std. dev.	Al	Std. dev.	Ru	Std. dev.
	Overall	51.8	1.1	47.8	1.3	0.4	0.08
	Plain -1	46.9	1.5	52.4	1.7	0.7	0.08
	Striped -2	49.5	1.0	50.1	1.2	0.4	0.07
	Light phase -3	45.0	1.7	48.6	1.3	6.4	1.0
TiAl-Pt		Ti	Std. dev.	Al	Std. dev.	Pt	Std. dev.
	Overall	51.3	1.1	47.3	1.1	1.4	0.4
	Plain- 1	50.1	1.2	47.8	1.1	2.1	1.5
	Striped -2	52.0	1.0	45.9	0.7	2.1	0.8
	Light phase-4	45.2	1.7	49.3	2.0	5.6	1.2
TiAl-Ir		Ti	Std. dev.	Al	Std. dev.	Ir	Std. dev.
	Overall	51.8	1.2	47.4	1.1	0.8	0.5
	Plain 1	48.7	0.9	50.4	1.3	0.9	0.5
	Striped 2	52.6	0.8	47.1	0.4	0.3	0.1
	Light phase-3	47.3	1.5	48.9	1.5	3.8	1.0
TiAl-Ag		Ti	Std. dev.	Al	Std. dev.	Ag	Std. dev.
	Overall	52.0	0.8	47.7	0.6	0.3	0.2
	Plain 1	46.3	0.7	53.5	0.6	0.7	0.2
	Striped 2	52.0	0.8	47.6	0.8	0.4	0.3
	Light phase-3	47.6	0.4	44.3	1.3	10.42	2.0

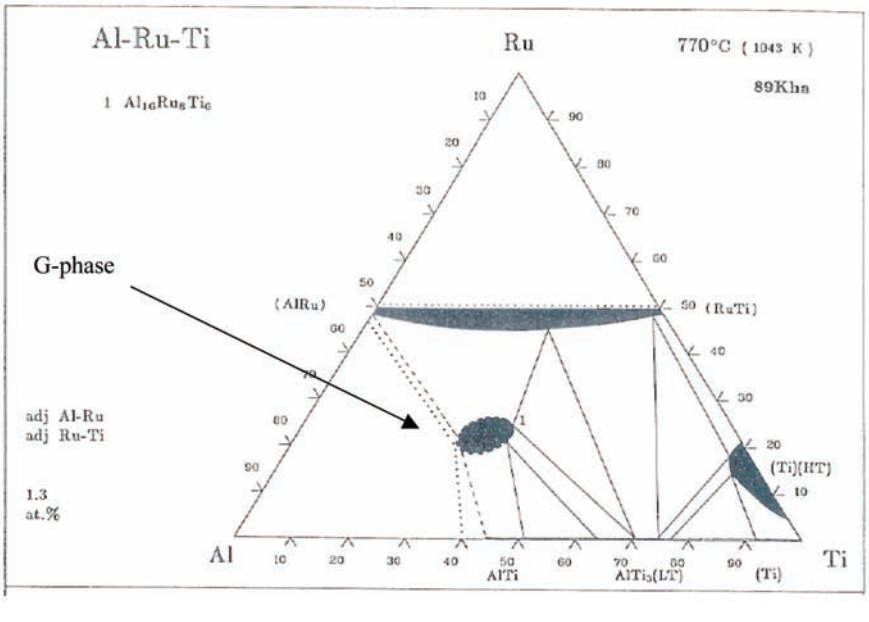

Figure 7—Isothermal section of the ternary Ti-Al-Ru phase diagram[14]

compound with the $Mn_{23}Th_6$ structure, a *D*8a-type crystal structure with a complex unit containing 116 atoms based on a bcc structure[12].

Effect of precious metal content on the microstructure of TiAl compounds

The increase of PM content led to an increase in the precipitation of the new phase at grain boundaries. This precipitation progressed more in the γ grains as shown in Figure 8. The new phase developed between lamellar grains in the γ phase, resulting in a complete separation of lamellar grains. As the content of PMs increased, white phases of higher PM content formed at the centre (Figure 8b). At 2 at.% PM addition, the white phase, viewed at high magnification, showed a eutectic morphology (Figure 9).

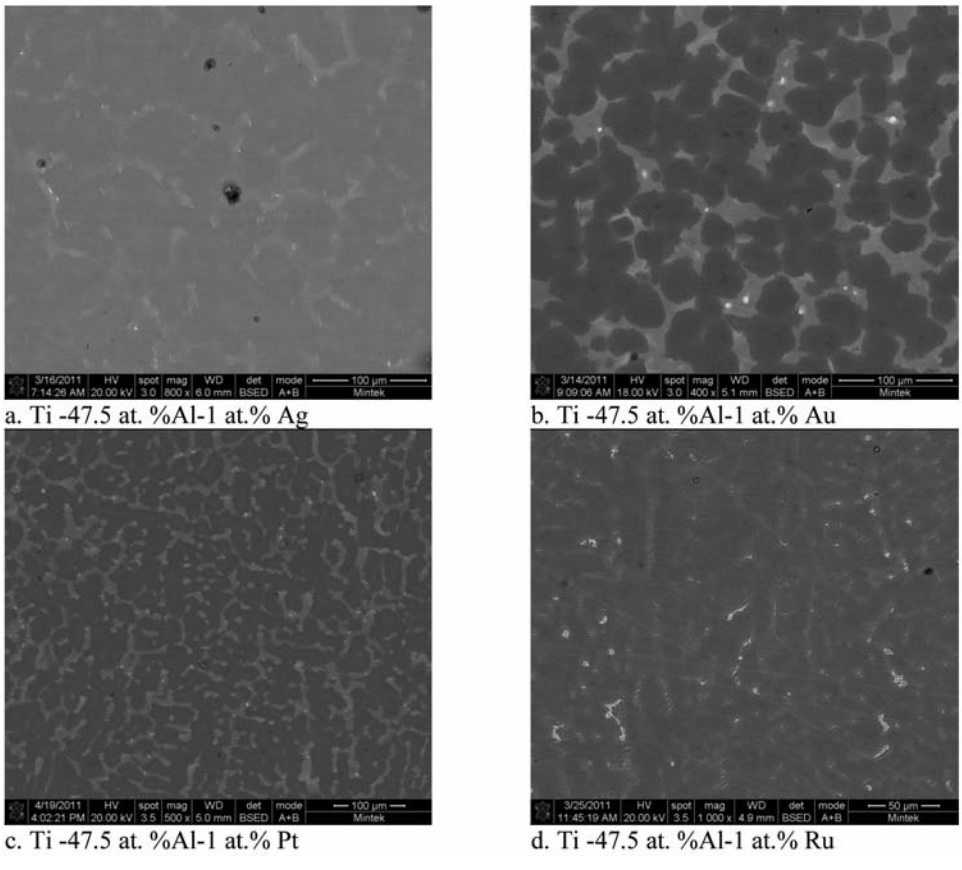

Figure 8—SEM mode micrographs of TiAl alloys with 1.0 at.% precious metal

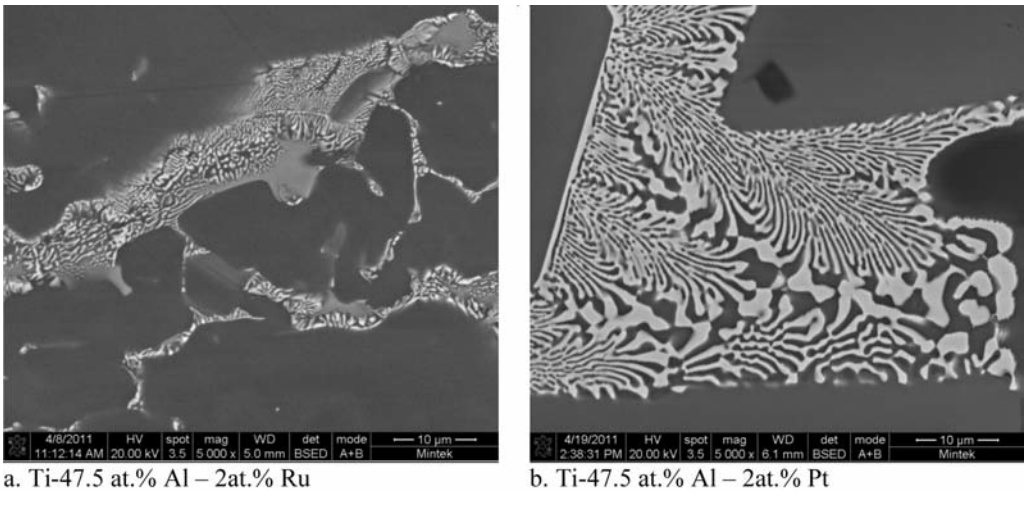

Figure 9—SEM mode micrographs of TiAl alloys with precious metals showing eutectic-like structures

Hardness evaluation

Hardness of TiAl alloys with 0.2 at.% precious metals

The Vickers hardness of the as-cast and heat-treated samples was evaluated and the results are reported in Table IV. The Vickers hardness of the plain TiAl was around 300, and the introduction of PMs resulted in a slight increase. However, the addition of silver resulted in a significant increase of the hardness, about 400HV_{10} in the as-cast condition. More investigation is needed to understand the sudden hardness increase observed in the Ag-containing TiAl alloys.

In general, the heat treatment at 1 000°C for 1 hour resulted in a slight softening of the alloys. Samples that had the highest hardness in the as-cast condition, TiAl-Pd and TiAl-Ag, showed the largest decrease. The decrease in hardness was expected, as the heat treatment was to soften the TiAl-based alloys while keeping the as-cast microstructure. To ensure that, the heat treatment temperature was set to correspond to annealing, without phase change, using the Ti-Al phase diagram[12,15].

Effect of precious metal content on the hardness of the TiAl alloys

The increase of PM content was assessed for its effect on the hardness, and the results are given in Table V. The macro-hardness of the TiAl alloys showed a general decreasing trend with increasing PM content (Figure 10), although it remained in the same range observed at the addition level of 0.2 at.% PMs, that is, 280-380HV_{10}. However, TiAl alloys with Pd and Ir showed an inverse trend.

Oxidation behaviour of plain and precious metals-containing TiAl at high temperatures

TiAl with addition of 0.2 at.% precious metals

The high-temperature behaviour of the alloys was assessed by thermogravimetric analysis (TGA) with the results shown in Figures 11 and 12 together with those from a TiAl powder obtained by mechanical alloying. At 1 185°C in air, the weight gain in TiAl alloys containing 0.2 at.% PMs varied between 1 and 2 percent, with Ir- and Pt-containing TiAl alloys showing the highest weight gain (~2 percent) and Ru- and Pd-containing TiAl the lowest weight gain (~1 percent). This is illustrated in Figure 12, which is an expansion of the curves in Figure 11. In general, as the temperature increased, the TiAl alloys with PMs showed an abrupt weight increase from around 950°C, below which the weight gain was less than 1 percent in almost all cases. When compared to the weight gain in plain TiAl (Figure 11), the weight gains in TiAl alloys containing precious metals were significantly small. The weight gain in plain TiAl started earlier (~36 percent at 950°C), and showed an abrupt increase at about 480°C.

These results indicated that the presence of 0.2 at.% precious metals in the alloys retarded oxygen pick-up and therefore oxidation, and demonstrated that by adding

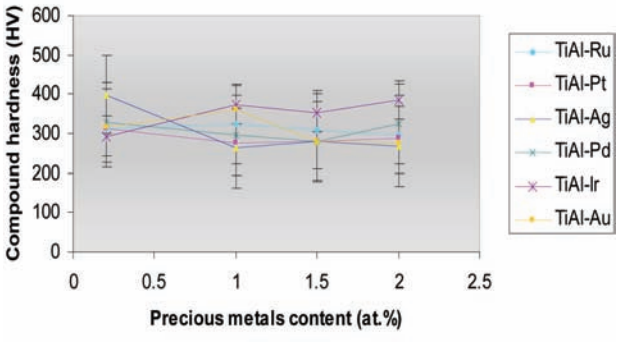

Figure 10—TiAl alloy macrohardness-precious metal content relationship

Table IV

Vickers macro-hardness of TiAl alloys with 0.2 at.% precious metals

Condition	Parameter	Compound						
		TiAl	TiAl-Ru	TiAl-Pd	TiAl-Pt	TiAl-Ir	TiAl-Ag	TiAl-Au
As-cast	Macro-hardness HV_{10}	281	314	328	314	293	399	318
	Standard deviation	23	28	23	10	17	13	22
Heat Treated	Macro-hardness HV_{10}	269	303	311	298	300	375	308
	Standard deviation	25	11	18	14	12	9	19

Table V

Vickers macro-hardness of as-cast plain and PMs-containing TiAl alloys

P.M. content (at.%)	Parameter	Compound					
		TiAl-Ru	TiAl-Pd	TiAl-Pt	TiAl-Au	TiAl-Ag	TiAl-Ir
1	Macro-hardness HV_{10}	324	296	276	362	264	373
	Standard deviation	17	16	11	14	9	15
1.5	Macro-hardness HV_{10}	309	280	281	280	281	353
	Standard deviation	33	21	15	14	10	11
2	Macro-hardness HV_{10}	298	326	289	277	268	385
	Standard deviation	27	14	16	13	8	16

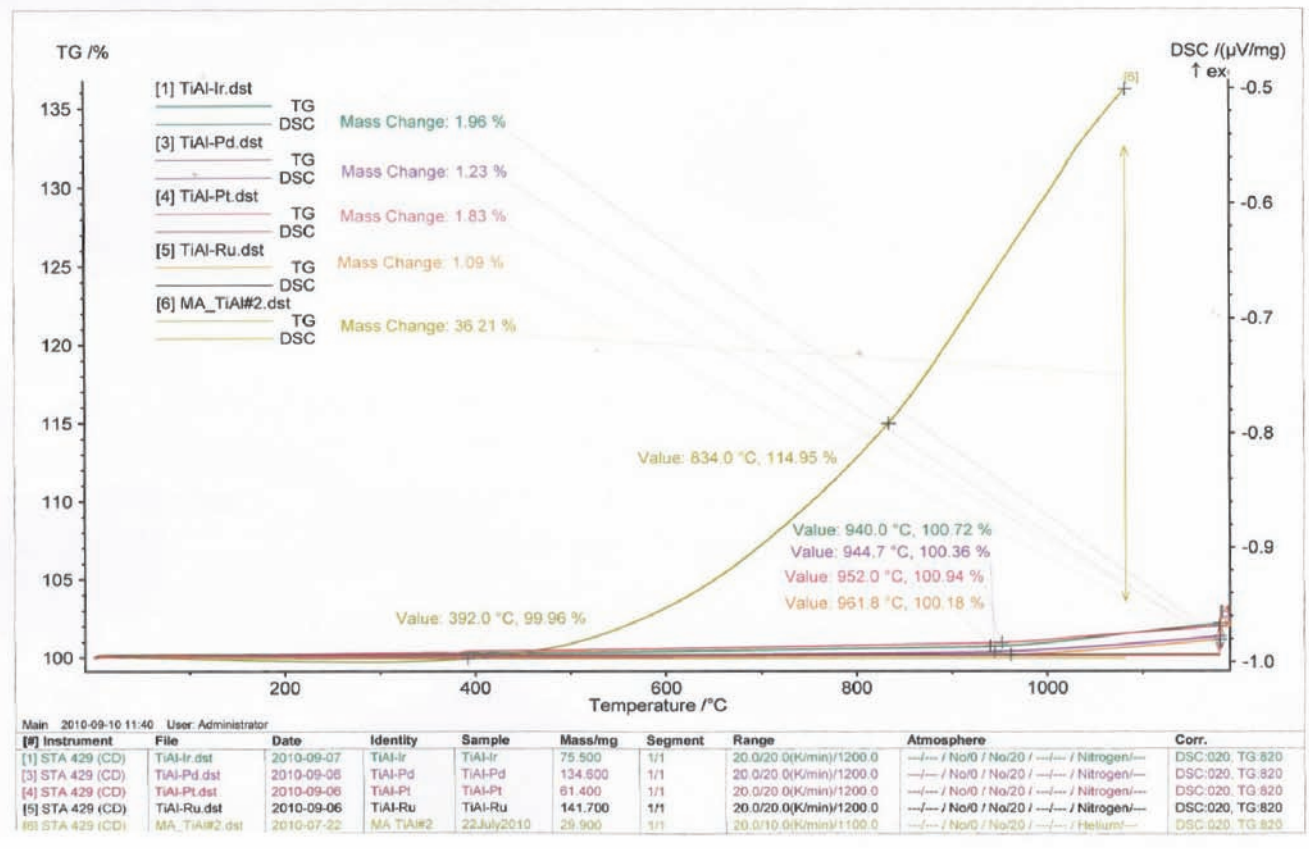

Figure 11—TGA curves of plain and TiAl alloys with 0.2 at.% PMs, including mechanically alloyed powder

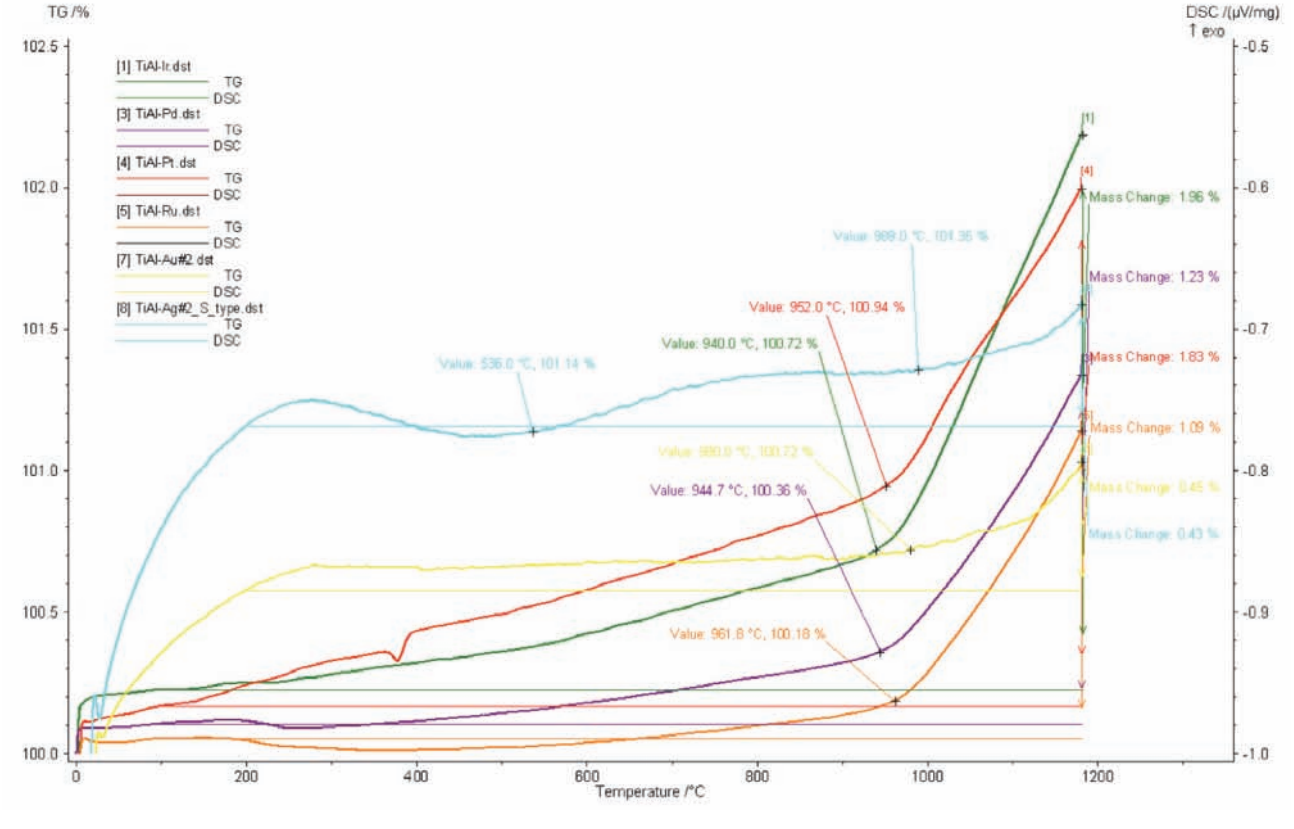

Figure 12—Typical TGA curves of TiAl alloys with 0.2at.% precious metals

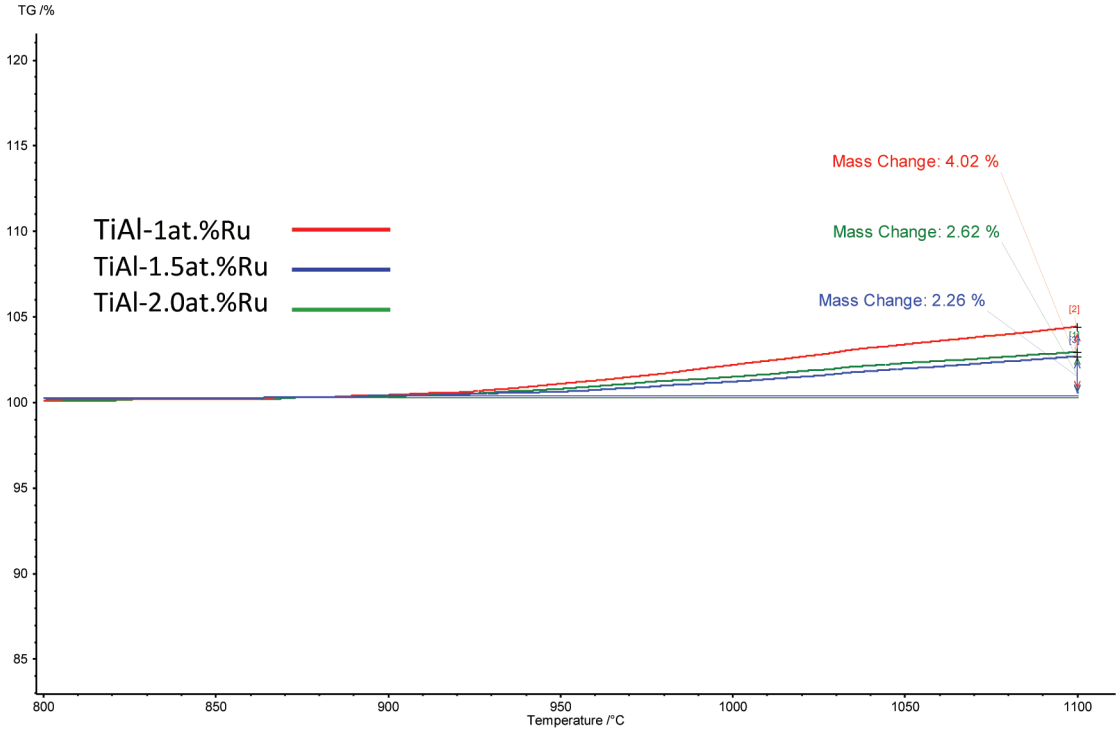

Figure 13—Typical TGA curves of TiAl alloys containing 1, 1.5 and 2 at.% Ru

Table VI

Mass change as a function of PM content at 1 185°C

PM content (at.%)	Relative mass change in TiAl compound doped with precious metal (%)					
	Ru	Pd	Pt	Ag	Au	Ir
0.2	1.09	1.23	1.83	0.93	0.45	1.96
1.0	4.02	0.85	1.32	2.84	2.14	0.97
1.5	2.26	0.57	2.28	1.42	4.65	0.53
2.0	2.62	0.90	2.18	1.41	9.44	1.13

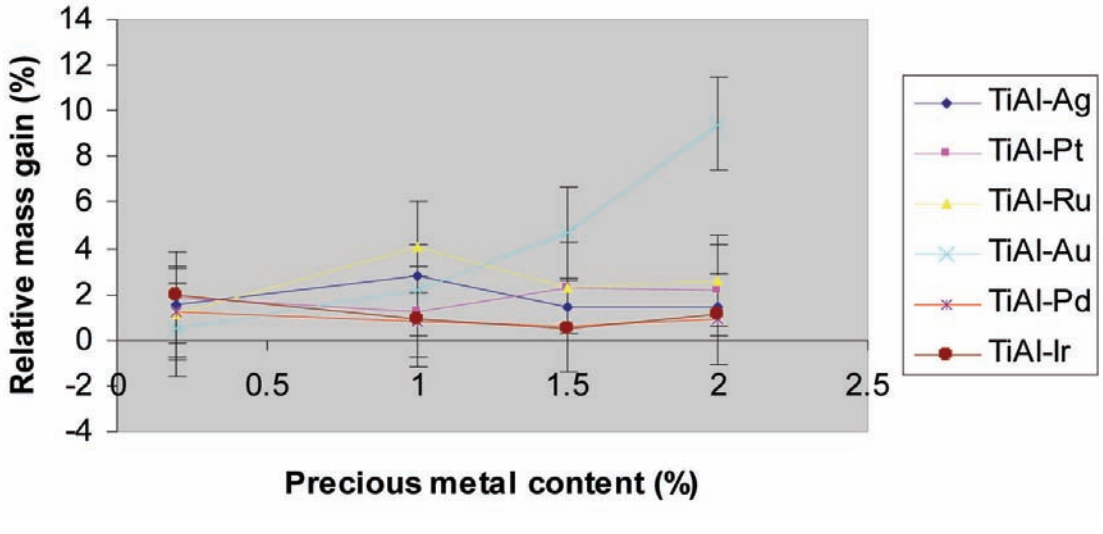

Figure 14—Typical curves of mass gain as functions of PM contents in TiAl alloys at 1 185°C

precious metals, the oxidation resistance of the TiAl can be significantly improved.

Effect of precious metal content on the oxidation behaviour of the TiAl alloys

The effect of PM content on the oxidation behaviour of TiAl was also assessed by a thermogravimetric analysis (TGA) of samples with 1, 1.5 and 2 at.% PMs. A typical TGA curve is shown in Figure 13 for the Ru-containing TiAl alloy. Table VI summarizes the mass gains for different PM contents. The mass gain at higher PM content (1–2 at.%) was either the same or higher than the mass gain observed with TiAl containing only 0.2 at.% PM, and is shown in Figure 14, for the mass gain at 1 185°C. For the gold-containing TiAl alloy, which showed a mass gain of about 9.5 percent at an addition level of 2 at.% Au, the increase was greater. These observations indicated that increasing the content of PMs in the TiAl alloy did not give better oxidation resistance than TiAl containing 0.2 at.% PMs, and the best results should be achieved below 1 at.% PM addition.

Conclusion

Plain and precious metals-containing TiAl alloys were produced by melting commercial aluminium and titanium together to the composition of Ti-47.5 at.% Al with additions of precious metals (PMs) at 0.2, 1, 1.5, and 2 at.%. The TiAl alloys were characterized in as-cast and heat-treated conditions in terms of their microstructure, hardness, and oxidation behaviour.

It was found that at Ti-47.5 at.% Al, the microstructure of plain TiAl alloy was duplex, consisting of lamellar and γ grains. The lamellar grains consisted of lamellae of γ (TiAl) and α_2 (Ti_3Al), with an overall composition of Ti-(43-47) at.% Al. The γ grains consisted of γ phase with an aluminium content above 50 at.%.

The addition of PMs to TiAl alloys at 0.2 at.% resulted in the formation of a new phase, mainly at the grain boundaries and in the γ grains, without major change in the matrix.

The hardness of the plain alloy was around $300HV_{10}$. Addition of PMs at 0.2 at.% to TiAl alloys resulted in a slight increase in hardness, and significant improvement of the oxidation resistance.

Increasing the PM content from 0.2 at.% to 1, 1.5 and 2 at.% resulted in increased precipitation of the whiter phase with high content of PMs, with no significant change to the hardness and no improvement to oxidation resistance. Instead, the addition of PMs above 1 at.% appeared to be deleterious to the oxidation resistance. Precious metal addition above 1 at.% resulted in the precipitation of the new phase at grain boundaries, which developed subsequently in the γ phases and isolated lamellar grains.

Acknowledgement

This paper is published with the permission of Mintek. The DST-AMI-PMDN, Mintek, Mr Edson Muhuma and Mr. Mokae Bambo at Mintek are thanked. L.A. Cornish thanks the National Research Foundation and the department of Science and Technology.

References

1. Tetsui, T. and Miura, Y. Heat-resistant cast TiAl alloy for passenger vehicles. *Mitsubishi Heavy Industries Ltd., Technical Review*, vol. 39, no. 1, 2002. pp. 1–9.
2. Duarte, A., Viana, F., and Santos, H.M.C.M. As-cast titanium aluminides microstructure modification, *Materials Research*, vol. 2–3, 1999. pp. 191–195.
3. Kimura, Y. and Pope, D. Ductility and toughness considerations in intermetallics, Structural intermetallics. The *Minerals, Metals & Materials Society*. 1997. pp. 99–106.
4. Jovanović, M.T., Dimčić, B., Bobić, I., Zec S. and Maksimović, V. Microstructure and mechanical properties of precision cast TiAl turbocharger wheels, *Materials Processing Technology*, 2004. 167. pp.
5. Chu, M.S. and Wu, S.K. The improvement of high temperature oxidation of Ti-50Al by sputtering Al film and subsequent interdiffusion treatment, *Acta Materialia*, vol. 51, 2003. pp. 3109–3120.
6. Ramanujan, R.V. Phase transformations in γ-based titanium aluminides, *International Materials Reviews*, vol. 45, no. 6, 2000. pp. 217–240.
7. Goral, M., Moskal, G., and Swadzba, L. The influence of Si on oxidation resistance of aluminide coatings on TiAl alloy, *Journal of Achievement in Materials and Manufacturing Engineering*, vol. 18, 2006. pp. 459–462.
8. Moskal, G. Microstructure and oxidation behaviour of TiAlSi coatings on TiAlCrNb alloy, *Journal of Achievements in Materials and Manufacturing Engineering*, vol. 20, 2007. pp. 263–266.
9. Huang, S.C. and Chesnutt, J.C. Gamma TiAl and its alloys, *Intermetallic compounds*, vol. 2, John Wiley & Sons Ltd, 1994. pp. 73–89.
10. Niewolak, L., Shemet, V., Thomas, C., Lersch, P., Singheiser, L., and Quadakkers, W.J. Oxidation behaviour of Ag-containing TiAl-based intermetallics, *Intermetallics*, vol. 12, 2004. pp. 1387–1396.
11. Calaphad. The titanium-aluminum (Ti-Al) phase diagram calculated with Thermo-Calc software, coupled with SSOL2 thermodynamic database, http:// www.calphad.com/titanium-aluminum.html. (Accessed 22 June 2011).
12. Khataee, A., Flower, H.M., and West, D.R.F. The alloying of titanium aluminides with ruthenium, *Platinum Metals Review*, vol. 33, no. 3, 1989. pp. 106–113.
13. Villars, P., Prince, A., and Okamoto, H. Handbook of Ternary Alloy Phase Diagrams. ASM International, vol. 4. pp 4273–4278
14. Murray, J.L. Calculation of the titanium-aluminium phase diagram. *Metallurgical Transactions A*, vol. 19A, 1988. pp 243–247. ◆